Available online at www.sciencedirect.com
SCIENCE DIRECT®
Materials Letters 58 (2003) 172–175
MATERIALS LETTERS
www.elsevier.com/locate/matlet

Elastic modulus of porous Ce-TZP ceramics

L.F.C.P. Lima*, A.L.E. Godoy, E.N.S. Muccillo

Centro Multidisciplinar para o Desenvolvimento de Materiais Cerâmicos, CCTM-Instituto de Pesquisas Energéticas e Nucleares, C. P. 11049-Pinheiros, 05422-970, S. Paulo, SP, Brazil

Received 23 January 2003; received in revised form 28 April 2003; accepted 2 May 2003

Abstract

The elastic modulus of tetragonal zirconia polycrystals doped with cerium (Ce-TZP) ceramics with a range (~ 5 to ~ 35%) of porosity was measured at room temperature by dynamic mechanical analysis (DMA). Bar-shaped specimens with varying pore volume fractions were prepared using different processing procedures. The as-sintered bars without any surface finishing were used for measurement in the three-point bending configuration. Results show that the elastic modulus decreases linearly with increasing porosity. The main conclusion is that the dynamic mechanical analysis may be useful as an alternative technique for the study of elastic modulus–porosity relation in ceramic materials.

PACS: 62.20.F; 81.20.W; 81.05.R; 81.40
Keywords: Ce-TZP; Elastic properties; Porosity; Microstructure; Characterisation methods

1. Introduction

Zirconia-based ceramics have been extensively investigated due to their attractive mechanical, electrical, and thermal properties. Tetragonal zirconia polycrystals doped either with yttrium (Y-TZP) or cerium (Ce-TZP) have received great attention because of their high thermomechanical properties. Ce-TZP ceramics have high fracture toughness and high thermal stability compared to Y-TZP ceramics [1].

The mechanical properties of engineering ceramics are largely dependent upon their microstructures that are, by their turn, determined by the specific processing routes employed to fabricate these materials [2,3]. The presence of small defects such as pores can lead to a drastic decrease in strength value, in the elastic modulus, and in fracture toughness [4].

Several studies have been carried out over the past years to derive reliable equations that describe the relationship between the relative density or porosity, and the elastic modulus of sintered materials [5–11]. In these studies, porous samples were prepared by sintering compacted powders to controlled levels of density, and their elastic moduli were determined. Three basic methods are usually utilised to measure the elastic modulus. The first involves direct measurement of strain as a function of stress. The second method is based on measurement of the resonance frequency of the material. The last method is based on ultrasonic techniques [12].

The main purpose of this work was to verify the use of dynamic mechanical analysis (DMA) as an alternative technique for the determination of the elastic modulus in porous ceramics. The present work was also undertaken to explore the relation between processing techniques and porosity in the sintered ceramics. The zirconia–ceria solid solution was selected for this study because of its inherent difficulty to attain full density, allowing for a wide range of densification in sintered compacts.

2. Experimental

In order to obtain sintered specimens with different degrees of densification, mechanically mixed and high-energy milled powders were used.

ZrO_2 (TZ0, Tosoh) and CeO_2 (99.9%) were used as starting materials for preparing mixed and milled powders. The cerium precursor was prepared at our Institute from a cerium-rich concentrate by the ion exchange resin and

* Corresponding author. Fax: +55-11-38169370.
E-mail address: lfilipe@ipen.br (L.F.C.P. Lima).

0167-577X/$ - see front matter © 2003 Elsevier B.V. All rights reserved.
doi:10.1016/S0167-577X(03)00439-7

fractional precipitation techniques. The nominal composition was set to 12 mol% CeO_2.

The mechanical mixing of zirconia and ceria powders was performed in a mixer (Turbula, model T2C) for 6 h using zirconia balls, and with absolute ethanol as dispersing medium. The high-energy milling was carried out in a vibratory mill (Spex, model 8000) with stabilized zirconia vial and balls for 4 h, and using a ball-to-powder mass ratio of 3:1.

Before compaction, a binder material (polyvinyl alcohol, MW = 72,000) was added (1–2 wt.%) to the powders. Bar-shaped specimens (60 × 12 × 3 mm) were formed by uniaxial compaction in a stainless steel die. The pressed bars were heat treated at 700 °C for 1 h in air for binder burnout, and then sintered at 1500 °C for times ranging from 1 to 4 h.

The apparent density of sintered specimens was determined by using the Archimedes principle in distilled water. The volume fraction of pores (p), or porosity, is defined by $p = 1 - \rho/\rho_{th}$, where $\rho_{th}$is the theoretical density of the material and ρ is the apparent sintered density. In the present study, ρ_{th} for zirconia–12 mol% ceria was taken as 6.22 g cm^{-3}, which is an average of the several values reported for this composition in the literature varying from 6.14 [13] to 6.29 [14]. The morphology of powder particles was observed by scanning electron microscopy (SEM; Philips, model XL30). The particle size distribution was measured by laser scattering (Cilas granulometer, model 1064) using sodium pyrophosphate as dispersing agent. Mercury porosimetry (Micromeritics, Autopore III) was measured on selected sintered specimens. The elastic modulus (E) was measured by dynamic mechanical analysis (Netzsch, model 242) in the flexural (three-point bending) configuration at room temperature. For this measurement, sintered bar-shaped specimens were used without any further treatment such as cutting to adjust linear dimensions or surface finishing.

3. Results and discussion

Particle size distribution of the two powders is shown in Fig. 1. The powder prepared by mixing of the starting oxide materials exhibits a typical sigmoid shape resulting from a good dispersion of the powder particles. The average particle size obtained at 50% mass finer is 0.95 μm. The milled powder presents a distorted sigmoid-shaped distribution curve. This is an indication that the powder particles could not be suitably dispersed during the process of sample preparation for this type of analysis. Considering that high-energy milling should produce small size particles, the actual average particle size may be smaller than the particle size shown in this figure. However, this particle size distribution does indicate the average degree of powder agglomeration in the milled powder. The high-energy milled powder exhibits a larger particle/agglomerate size and a wider particle size distribution than the mixed powder.

Fig. 2 shows SEM micrographs of the starting oxide materials (Fig. 2a and b) and those of mixed (Fig. 2c) and high-energy milled (Fig. 2d) powders. The zirconia and ceria powders were dissimilar. They were constituted by different-sized and different-shaped particles/agglomerates. The mixed powder presents nanosized and agglomerated particles, with uniform size. After milling, the degree of agglomeration increased although the size of the powder particles is more homogeneous. These SEM micrographs offer direct evidence of the agglomerated microstructure of the powders under consideration. The agglomeration is expected to occur in nanosized brittle materials due to the high intensity of adhesion forces acting on powder particles [15]. However, one cannot ascertain on the strength of the agglomerates only by means of these SEM micrographs. In other words, the agglomerates formed during the mixing and milling processes may either break up during the compaction step or may retain their identities in the compacted body.

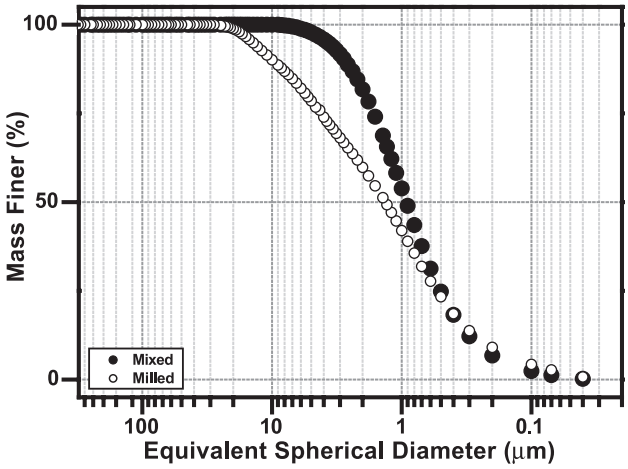

Fig. 1. Particle size distribution of mixed and milled powders.

Sintered bars prepared under different routes and different processing conditions presented a range of sizes (from 40 to 52 mm long, 8–10 mm large, and 1.2–3.7 mm thickness), and densification. The porosity varied from ~ 5% to ~ 35%. The most dense specimens were those prepared by mixing the starting oxide materials.

Besides the fracture of particles, high-energy milling of brittle materials may lead to phase transformation, crystallite size reduction, solid solution formation, phase amorphization, synthesis of new phases, and agglomeration. One possible explanation for the observed agglomeration is that it is due to the impacts of high-energy, which can compact clusters of particles giving rise to hard agglomerates [16]. Sintering of powder compacts containing hard agglomerates results in poor densification. In addition, the differential shrinkage of the compact can give rise to large pores in the sintered material.

A total of five sintered specimens prepared with the milled powder were selected for mercury intrusion experiments to obtain a better insight in the state of agglomeration produced by the high-energy milling process. A typical

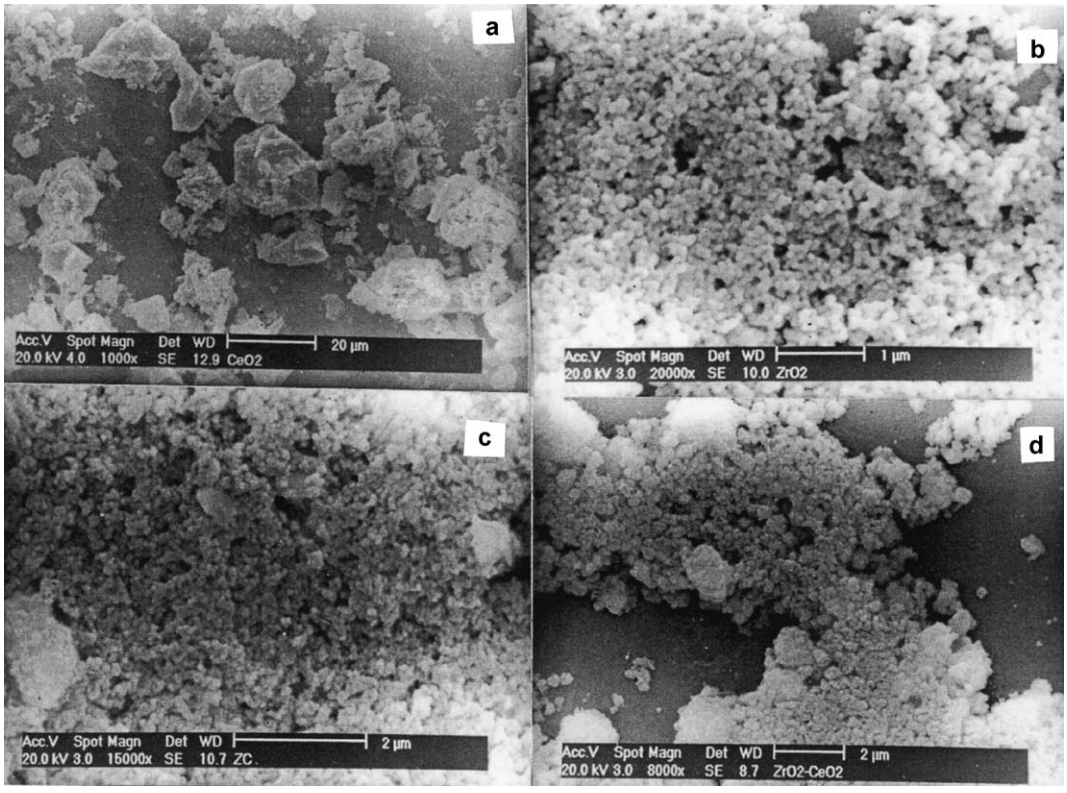

Fig. 2. SEM micrographs of starting materials (a and b), mixed (c), and milled (d) powders.

curve of cumulative volume per mass of specimen as a function of pore diameter is shown in Fig. 3. Two regions of mercury penetration are clearly resolved. The first one gives an average pore diameter of 1 μm, whereas the second stage has a maximum of about 0.01 μm. The shape of that curve is an indication that the milled powder contained hard agglomerates.

Fig. 4 shows the variation of the elastic modulus with the pore volume fraction measured by DMA on sintered compacts. A linear decrease of the elastic modulus with increasing porosity is observed in this figure. The elastic modulus varied from 17.5 to 144 GPa in the porosity range of study. Linear regression gives a correlation factor of 0.9685. Extrapolation to zero porosity gives an elastic modulus value equal to 162 GPa. This value is close to the literature data [1] for Ce-TZP ceramics. The relatively low r^2 value may result from the non-uniformization in the dimensions of bars before measurements. Moreover, the mixing and mill-

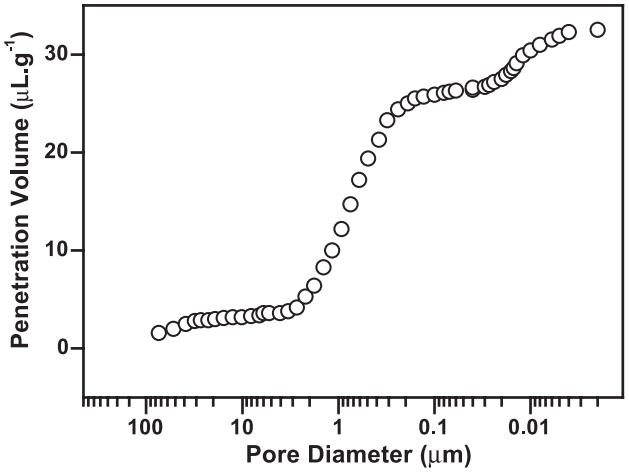

Fig. 3. Typical distribution of pore sizes obtained by mercury porosimetry in a sintered bar prepared from milled powder.

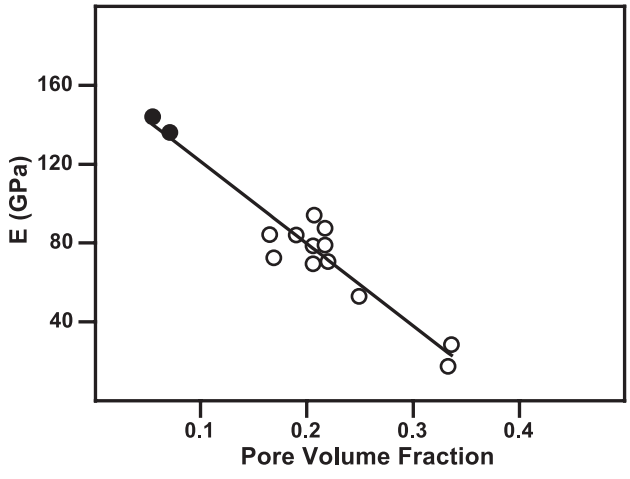

Fig. 4. Variation of the elastic modulus with porosity measured at room temperature by DMA at a frequency of 1 Hz. Sintered bars prepared from mixed (●) and milled (○) powders.

ing processes produced specimens with different fractions of open and closed porosities. The structure, size, and shape of pores were not taken into account in this work.

These results show that the DMA technique, which is most frequently used for the measurement of polymeric materials, may be useful for the study of the elastic modulus–porosity relation in ceramic materials.

4. Conclusions

Zirconia–ceria powders with different particle/agglomerate size distributions were prepared by mixing and high-energy milling of the starting oxide materials. The agglomerates formed in these processes are composed of nanosized particles. The high-energy milling gave rise to hard agglomerates resulting in poor densification of powder compacts. The elastic modulus of sintered Ce-TZP bars decreases with increasing pore volume fraction. These results suggest that the dynamic mechanical analysis may be a useful, fast, and low-cost technique for the study of the elastic modulus–porosity relation in ceramic materials.

Acknowledgements

To FAPESP (95/05630-2, 97/06152-2 and 99/04929-5), CNEN, CNPq (300934/94-7), and PRONEX for financial supports, and to T. C. Porfírio for the technical assistance.

References

[1] J.D. Cawley, W.E. Lee, Materials Science and Technology, A Comprehensive Treatment, Structure and Properties of Ceramics, vol. 11, VCH, Weinheim, Germany, 1994.
[2] F.F. Lange, J. Am. Ceram. Soc. 72 (1989) 3.
[3] R.W. Rice, Treatise on Materials Science and Technology, vol. 11, Academic Press, New York, 1977.
[4] R.W. Rice, Porosity of Ceramics, Marcel Dekker, New York, 1998.
[5] F.P. Knudsen, J. Am. Ceram. Soc. 42 (1959) 376.
[6] J.C. Wang, J. Mater. Sci. 19 (1984) 801.
[7] E.A. Dean, J.A. Lopez, J. Am. Ceram. Soc. 66 (1983) 366.
[8] K.K. Phani, S.K. Niyogi, J. Mater. Sci. 22 (1987) 257.
[9] K.K. Phani, J. Mater. Sci. 31 (1996) 262.
[10] J. Kovacik, J. Mater. Sci. Lett. 20 (2001) 1953.
[11] M. Asmani, C. Kermel, A. Leriche, M. Ourak, J. Eur. Ceram. Soc. 21 (2001) 1081.
[12] M. Bengisu, Engineering Ceramics, Springer, New York, 2001.
[13] A. Deptula, M. Carewska, T. Olczak, W. Lada, F. Croce, J. Electrochem. Soc. 140 (1993) 2294.
[14] E.N.S. Muccillo, D.M. Ávila, Ceram. Int. 25 (1999) 345.
[15] J.S. Reed, Introduction to the Principles of Ceramic Processing, Wiley Interscience, New York, 1995.
[16] W.J. Botta, D.E. Hanai, B.N. Santana, N.R. Oliveira Jr., R. Tomasi, Mater. Sci. Forum 179/181 (1995) 635.